A Radial Basis Function Galerkin Method for Inhomogeneous Nonlocal Diffusion[☆]

R. B. Lehoucq[a,*], S. T. Rowe[b]

[a] *Computational Mathematics, Sandia National Laboratories, Albuquerque, NM 87185-1320, USA*
[b] *Department of Mathematics, Texas A&M University, College Station, TX 77843-3368, USA*

Abstract

We introduce a meshfree discretization for a nonlocal diffusion problem using a localized basis of radial basis functions. Our method consists of a conforming radial basis of local Lagrange functions for a variational formulation of a volume constrained nonlocal diffusion equation. We also establish an L^2 error estimate on the local Lagrange interpolant. The stiffness matrix is assembled by a special quadrature routine unique to the localized basis. Combining the quadrature method with the localized basis produces a well-conditioned, sparse, symmetric positive definite stiffness matrix. We demonstrate that both the continuum and discrete problems are well-posed and present numerical results for the convergence behavior of the radial basis function method. We explore approximating the solution to inhomogeneous differential equations by solving inhomogeneous nonlocal integral equations using the proposed radial basis function method.

Keywords: Radial basis functions, nonlocal diffusion, Lagrange functions, volume constraint

1. Introduction

We introduce a meshfree discretization for a nonlocal diffusion problem using a localized basis of radial basis functions. Our approach builds upon and significantly extends the application of radial basis function methods for the nonlocal diffusion equation introduced in the proceedings paper [1]. We accomplish this by

[☆]The work of the authors was supported by the Laboratory Directed Research and Development (LDRD) program at Sandia National Laboratories. Sandia is a multi-program laboratory managed and operated by Sandia Corporation, a wholly subsidiary of Lockheed Martin Corporation, for the U.S. Department of Energy's National Nuclear Security Administration under contract DE-AC04-94AL85000

[*]Corresponding author

Email addresses: rblehou@sandia.gov (R. B. Lehoucq), srowe@math.tamu.edu (S. T. Rowe)

- introducing a conforming radial basis function method of N local Lagrange functions in contrast to the nonconforming basis of Lagrange functions used [1];
- demonstrating that the ensuing discrete volume-constrained nonlocal diffusion problem in $\mathbb{R}^n$ is well-posed by exploiting the results in the paper [2] established for the infinite dimensional problem;
- establishing an L^2 error estimate for the local Lagrange function interpolant;
- reducing the cost of computing the quadrature weights to the solution of N linear systems of order $O(\log N)^n$ from that of the $2N$ linear systems;
- demonstrating that the discretized inhomogeneous nonlocal diffusion is a good approximation of the classical diffusion problem as the region of nonlocality ε vanishes;

In particular, our approach maintains the same benefits of the radial basis function method proposed in [1] while avoiding the solution of the dense linear systems needed for the quadrature weights and determination of the thin plate spline coefficients in terms of the Lagrange functions—the solution of two linear systems of order N. Moreover, we extend the results of [1] by considering inhomogeneous nonlocal diffusion equations and demonstrating that both the continuum and discrete problems are well-posed by appealing to theory developed in [2].

Nonlocal diffusion generalizes classical diffusion by replacing the partial differential equations with integral equations. Various models have been proposed for these cases of so-called anomalous diffusion, which include models based on integral equations and fractional derivatives. The nonlocal equation we consider has applications in a variety of fields besides anomalous diffusion such as image analyses, nonlocal heat conduction, machine learning, and peridynamic mechanics. We apply our conforming radial basis method to a volume constrained diffusion equation. Volume constraints replace the boundary conditions associated with classical diffusion and are needed to demonstrate that the problem is well-posed and then allow a link with a Markov jump process; see [2, 3] for additional information and citations to the literature. Section 2 reviews nonlocal diffusion, its relationship with classical diffusion and its variational formulation.

Radial basis functions have been extensively studied for meshfree interpolation and approximation. Radial basis functions have also been applied in a variety of areas besides interpolation of scattered data on subsets $\mathbb{R}^n$. They have seen notable success in collocation methods for elliptic, parabolic, and hyperbolic partial differential equations. Section 3 briefly reviews the aspects of radial basis functions needed, including citations to the literature, and introduces the application of local Lagrange functions and a quadrature rule necessary for a practical numerical method. To the best of our knowledge, the application of these two techniques to finite domains in $\mathbb{R}^n$ is a novel contribution of our paper.

Section 4 introduces the simple modification of the local Lagrange functions rendering the novel conforming radial basis function method for nonlocal diffusion that is the primary contribution of our paper. Proposition 1 establishes an L^2 error estimate on the local Lagrange interpolant; the numerical experiments demonstrate that second order convergence is observed, in concordance with the error estimate. We also propose an approximation of the stiffness matrix via the quadrature rule introduced in Section 3.2 that results in a matrix containing the sparsity inherent in the integral operator. We also demonstrate that the resulting approximate stiffness matrix is symmetric positive definite given some mild conditions.

Numerical experiments for the discretization of the nonlocal diffusion problem are discussed in Section 5. In addition to studying the discretization of nonlocal diffusion problems, Section 5.3 presents experiments that consider approximating the solution to an inhomogeneous differential equation by discretizing and solving an inhomogeneous nonlocal diffusion problem.

1.1. Nonlocal vector calculus

The nonlocal vector calculus developed in [4] provides nonlocal analogues of the gradient, divergence, and curl operators. We quickly summarize the aspects of the nonlocal vector calculus required for the nonlocal diffusion equation; the calculus enables a concise formulation synergistic with conventional variational formulation of classical diffusion.

Let $\nu(x,y), \alpha(x,y) : \mathbb{R}^n \times \mathbb{R}^n \to \mathbb{R}^k$ where α is an anti-symmetric mapping, i.e., $\alpha(x,y) = -\alpha(y,x)$. The nonlocal divergence operator $\mathcal{D}$ acts on ν by

$$\big(\mathcal{D}\nu\big)(x) := \int_{\mathbb{R}^n} \big(\nu(x,y) + \nu(y,x)\big) \cdot \alpha(x,y)\, dy.$$

The adjoint operator $\mathcal{D}^* u$

$$\big(\mathcal{D}^* u\big)(x,y) = -\big(u(y) - u(x)\big)\alpha(x,y) \qquad \text{for } x, y \in \mathbb{R}^n\,,$$

and is derived from the inner product

$$\int_{\mathbb{R}^n} \big(\mathcal{D}\nu\big)(x)\, u(x)\, dx = \int_{\mathbb{R}^n} \int_{\mathbb{R}^n} \nu(x,y)\, \big(\mathcal{D}^* u\big)(x,y)\, dy\, dx\,.$$

For an open subset $\Omega \subset \mathbb{R}^n$, we define the interaction domain

$$\Omega_{\mathcal{I}} := \{y \in \mathbb{R}^n \setminus \Omega : \alpha(x,y) \neq 0 \text{ for some } x \in \Omega\} \tag{1}$$

representing the set of points that interact with points in Ω.

2. Variational formulation of nonlocal diffusion

We define the energy functional

$$E(u; f) := \frac{1}{2} \int_{\Omega\cup\Omega_{\mathcal{I}}} \int_{\Omega\cup\Omega_{\mathcal{I}}} \mathcal{D}^* u \cdot \big(\Theta \cdot \mathcal{D}^* u\big)\, dx\, dy - \int_{\Omega} f u\, dx$$

where f is a given function defined over Ω and Θ is a second-order tensor satisfying $\Theta(x,y) = \Theta^T(x,y) = \Theta(y,x)$. Let $E_c(u) := \int_{\Omega_{\mathcal{I}}} u(x)^2\,dx$ denote the constraint functional. We consider the minimization problem

$$\min E(u;f) \qquad \text{subject to} \qquad E_c(u) = 0.$$

The constraint functional may be interpreted as a nonlocal Dirichlet volume constraint analogous to a Dirichlet boundary condition. By considering test functions v that satisfy $E_c(v) = 0$, we arrive at the necessary conditions for the minimization problem: Find u such

$$\int_{\Omega\cup\Omega_{\mathcal{I}}} \int_{\Omega\cup\Omega_{\mathcal{I}}} \mathcal{D}^*u \cdot \big(\Theta \cdot \mathcal{D}^*v\big)\,dy\,dx = \int_{\Omega} f\,v\,dx \tag{2}$$

holds for all v. To derive the strong form of the above variational problem, we use the nonlocal Green's first identity

$$\int_{\Omega} v\mathcal{D}\big(\Theta\cdot\mathcal{D}^*u\big)\,d\,x - \int_{\Omega\cup\Omega_{\mathcal{I}}}\int_{\Omega\cup\Omega_{\mathcal{I}}} \mathcal{D}^*u\cdot\big(\Theta\cdot\mathcal{D}^*v\big)\,dy\,dx = \int_{\Omega_{\mathcal{I}}} v\,\mathcal{N}\big(\Theta\cdot D^*u\big)\,dx\,,$$

where the interaction operator $\mathcal{N}(\nu):\mathbb{R}^n\to\mathbb{R}$ is defined by

$$\mathcal{N}(\nu)(x) := -\int_{\Omega\cup\Omega_{\mathcal{I}}} \big(\nu(x,y)+\nu(y,x)\big)\cdot\alpha(x,y)\,dy \qquad \text{for } x\in\Omega_{\mathcal{I}}\,,$$

to rewrite (2). Since v satisfying the constraint $E_c(v)=0$ is arbitrary, we have formally established that

$$\begin{cases} \mathcal{L}u = f & \text{on } \Omega, \\ u = 0 & \text{on } \Omega_{\mathcal{I}}\,, \end{cases} \tag{3a}$$

is the classical formulation of the variational problem (2) where

$$\mathcal{L}u = \int_{\Omega\cup\Omega_{\mathcal{I}}} \mathcal{D}^*u\cdot\big(\Theta\cdot\mathcal{D}^*u\big)\,dy\,, \tag{3b}$$

or as an integral operator

$$\mathcal{L}u(x) = \int_{\Omega\cup\Omega_{\mathcal{I}}} \big(u(y)-u(x)\big)\alpha(x,y)\cdot\big(\Theta(x,y)\alpha(x,y)\big)\,dy\,, \quad x\in\Omega\,. \tag{3c}$$

2.1. Abstract Variational Problem

In contrast to the classical diffusion model that imposes boundary conditions, the nonlocal model enforces conditions over a positive measure volume, or a volume constraint. This constraint is the key to demonstrating that the weak formulation of (3) is well-posed. We briefly review the results in [2] providing

conditions on the kernel $\gamma = \alpha \cdot \Theta \cdot \alpha$ so that the nonlocal diffusion equation is well-posed. Suppose that the kernel satisfies the following conditions:

$$\gamma(x,y) \geq 0 \quad \forall y \in B_\varepsilon(x) \text{ and } \gamma(x,y) \geq \gamma_0 > 0 \ \ \forall y \in B_{\varepsilon/2}(x)\,, \tag{4a}$$

$$\gamma(x,y) = 0 \quad \forall y \in (\Omega \cup \Omega_I) \backslash B_\varepsilon(x)\,, \tag{4b}$$

for a sphere $B_\varepsilon(x)$ of finite radius ε centered at x, and assume there exist positive constants γ_1 and γ_2 so that

$$\gamma_1 \leq \int_{(\Omega\cup\Omega_I)\cap B_\varepsilon(x)} \gamma(x,y)\,dy\,, \quad \int_{\Omega\cup\Omega_\mathcal{I}} \gamma^2(x,y)\,dy \leq \gamma_2^2 \qquad \forall\, x \in \Omega\,. \tag{4c}$$

Let $\Omega \subset \mathbb{R}^n$ be an open region and let $\Omega_\mathcal{I}$ be the interaction domain corresponding to Ω, as defined in (1). Let $u, v \in L^2(\Omega \cup \Omega_\mathcal{I})$, $f \in L^2(\Omega)$. We define the bilinear form $a(\cdot,\cdot)$

$$a(u,v) := \frac{1}{2} \int_{\Omega\cup\Omega_\mathcal{I}} \int_{\Omega\cup\Omega_\mathcal{I}} \mathcal{D}^* u \cdot \big(\Theta \cdot \mathcal{D}^* u\big)\, dy\, dx. \tag{5}$$

The nonlocal bilinear form induces a semi-norm $|||u||| = \sqrt{a(u,u)}$ on $L^2(\Omega \cup \Omega_\mathcal{I})$, which is equivalent to the $L^2(\Omega \cup \Omega_\mathcal{I})$ norm for functions restricted to the constrained energy space

$$L^2_c(\Omega \cup \Omega_\mathcal{I}) := \{u \in L^2(\Omega \cup \Omega_\mathcal{I}) : |||u||| < \infty \text{ and } u|_{\Omega_\mathcal{I}} = 0 \text{ a.e.}\}.$$

Our abstract variational problem is: Find $u \in L^2_c(\Omega \cup \Omega_\mathcal{I})$ such that

$$a(u,v) = \int_\Omega f\, v\, dx \qquad \forall\, v \in L^2_c(\Omega \cup \Omega_\mathcal{I})\,. \tag{6}$$

The authors of the paper [2] demonstrate the coercivity and continuity of the bilinear form on $L^2_c(\Omega \cup \Omega_\mathcal{I})$ and the continuity of the linear form on the right hand-side of (6) imply that the variational problem is well-posed by the Lax-Milgram theorem.

Since our interest is in the inhomogeneous nonlocal diffusion equation, we consider symmetric kernels

$$\gamma(x,y) := \big(\kappa(x) + \kappa(y)\big)\Phi_\varepsilon(\|x-y\|), \tag{7}$$

where κ and Φ_ε are such that the conditions (4) are satisfied, where the radial function Φ_ε is compactly supported on a ball of radius ε. The results of [2] then imply that as $\varepsilon \to 0$, the solution u_ε of (3) converges to the solution of

$$\begin{cases} \nabla \cdot \kappa \nabla u = f & \text{on } \Omega \\ \qquad\quad u = 0 & \text{on } \partial\Omega\,. \end{cases} \tag{8}$$

The interested reader should also consult [2] for further details on nonlocal operators, comparisons between nonlocal diffusion and classical diffusion equations, and comparisons with the classical vector calculus and the nonlocal calculus. The recent paper [5] discusses the nonlocal analogue of (8) with a Neumann boundary condition and relationship with a smoothed particle hydrodynamic approximation.

2.2. Discrete Variational Problem

Let $V_h = \text{span}\{\phi_i\}_{i=1}^N \subset L_c^2(\Omega \cup \Omega_{\mathcal{I}})$ be a finite-dimensional subspace. The resulting discrete problem for (6) is: Find $u_h = \sum_{i=1}^N c_i \phi_i \in V_h$ such that

$$a(u_h, \phi_i) = \int_\Omega f\, \phi_i \, dx \qquad \forall\, \phi_i \in V_h\,. \tag{9}$$

The resulting linear system of order N

$$\mathbf{A}\boldsymbol{c} = \boldsymbol{f}$$

has matrix and vector entries given by $\mathbf{A}_{i,j} = a(\phi_i, \phi_j)$, $\boldsymbol{c}_i = c_i$, and $\boldsymbol{f}_i = \int_\Omega f\, \phi_i \, dx$. In Section 4, we present a conforming discretization using a localized basis of radial basis functions that generates a well-conditioned, sparse stiffness matrix. Because the bilinear form $a(\cdot,\cdot)$ is coercive and symmetric, $\mathbf{A}$ is a symmetric positive definite matrix.

3. Radial Basis Functions

Radial basis functions (RBFs) are used to construct the approximation space for the Galerkin method we propose in Section 4. Let $\Omega \subset \mathbb{R}^n$ and $\Phi : \Omega \to \mathbb{R}$ be a continuous function. We say that Φ is *radial* if there exists $\varphi : \mathbb{R}^+ \to \mathbb{R}$ such that $\Phi(x) = \varphi(\|x\|)$ for all $x \in \mathbb{R}^n$. Let $\{x_i\}_{i=1}^N = X \subset \Omega$ be a collection of scattered points, referred to as centers. A set of *radial basis functions* $\{\Phi_i\}_{i=1}^N$ is constructed by setting $\Phi_i(x) = \Phi(x - x_i) = \varphi(\|x - x_i\|)$.

The geometry of the centers is important for estimating the approximation quality of the RBF interpolant and for estimating the condition number of the interpolation matrix. RBF interpolation offers the advantage of not requiring regular distributions of points; arbitrarily scattered centers produce invertible interpolation matrices for positive definite functions. Let $X \subset \Omega \subset \mathbb{R}^n$ be a set of scattered centers. We define the *mesh norm* (or fill distance) h to be the radius of the largest ball in Ω that does not contain any centers and we define the *separation radius* q to be the minimal pairwise distance between the centers. See Figure 1 for a depiction of the mesh norm. These quantities are defined by

$$h = \sup_{x\in\Omega} \min_{x_j \in X} \|x - x_j\|, \qquad q = \min_{x_i, x_j \in X} \|x_i - x_j\|, \qquad \rho = \frac{h}{q}, \tag{10a}$$

where the *mesh ratio* ρ provides a means of judging how well distributed the points are. Informally, for ρ near one, the centers are almost uniformly distributed and large ρ indicates clustering of centers. We say that collections of centers $\{X_{h,q}\}$ are *quasi-uniformly* distributed if there exists positive constants C_1, C_2 such that

$$C_1 q \le h \le C_2 q. \tag{10b}$$

Geometrically, this condition controls how the centers cluster as the density of points increases. We note that for the quasi-uniformly distributed collections of centers $\{X_{h,q}\}$, we do not require that any of the point sets are nested in another. The interested reader should consult [6] or [7] for further details on radial basis functions and interpolation.

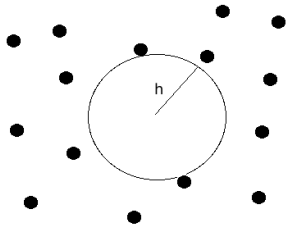

Figure 1: The mesh norm is the radius of the largest ball that does not contain any centers.

3.1. Local Lagrange Functions

We now discuss the construction of local Lagrange functions that are constructed more efficiently than the full Lagrange basis we used previously in [1]. This leads to a significant reduction in computational cost as explained in Section 1. Local Lagrange functions were first introduced for use on the sphere [8] where decay properties and quasi-interpolation convergence rates were studied. The local Lagrange basis can be constructed in parallel by solving small (relative to the number of centers) linear systems. Recent work [9] has extended theoretical properties of the local Lagrange basis to compact domains in $\mathbb{R}^n$.

The construction of local Lagrange functions involves the addition of centers outside of the domain Ω that are included in a larger set of points $\Xi \supset X$. Let

$$\tilde{\Omega} = \{x \in \mathbb{R}^n : d(x, \Omega) \leq Mh|\log h|\},$$

for a positive constant M. A set of centers Ξ can be constructed such that $\Xi \cap \Omega = X$ and Ξ has mesh norm h in $\tilde{\Omega}$. For each $x_i \in X$, let

$$\Upsilon_i = \{y \in \Xi : d(x_i, y) \leq Mh|\log h|\}. \tag{11a}$$

The constant M is independent of h and can always be chosen, see [9, 8]. The size of $|\Upsilon_i|$, the number of points in Υ_i, can be estimated by using (10a), the separation radius q, and a volume estimate. If we apply quasi-uniformity (10b) and since every center is separated by at least q, we estimate

$$|\Upsilon_i| \leq \frac{\mu\big(B_{Mh|\log h|}(x_i)\big)}{\mu\big(B_q(x_i)\big)} \sim \frac{M^n h^n}{Cq^n}|\log h|^n \leq \tilde{C}\rho^n|\log n|^n, \tag{11b}$$

where μ denotes the volume of a set in $\mathbb{R}^n$. For a quasi-uniformly distributed sets of centers, the mesh ratio ρ (10a) is bounded above and below by constants. This key estimate (11b) demonstrates that constructing a local Lagrange function requires solving a linear system of order $O\big(\log N^n\big)$ as opposed to $O(N)$ for the full Lagrange functions.

The *local Lagrange function* centered at x_i is defined to be

$$b_i(x) := \sum_{j=1}^{|\Upsilon_i|} \alpha_j \varphi(\|x - x_j\|) + \sum_{l=1}^{L} \beta_l p_l(x) \tag{12a}$$

where $\text{span}\{p_l\}_{l=1}^{L}$ denotes the space of polynomials of degree less than or equal to L on $\mathbb{R}^n$, and for $2m > n$ the function

$$\varphi(r) := \begin{cases} r^{2m-n} & n \text{ is odd} \\ r^{2m-n} \log r & n \text{ is even} \end{cases} \tag{12b}$$

is a thin plate spline. The coefficients α_j and β_l are determined by the solution of the saddle point linear system

$$\begin{aligned} \delta_{i,j} &= \sum_{j=1}^{|\Upsilon_i|} \alpha_j \varphi(\|x_i - x_j\|) + \sum_{l=1}^{L} \beta_l p_l(x_i) && \text{for } i = 1, \ldots, |\Upsilon_i|\,, \\ 0 &= \sum_{j=1}^{|\Upsilon_i|} \alpha_j p_l(x_j) && \text{for } l = 1, \ldots, L\,. \end{aligned} \tag{12c}$$

Given the N centers in X, the ensuing N local Lagrange functions can be shown to satisfy the Kronecker delta property $b_i(x_j) = \delta_{i,j}$. Augmenting the thin plate splines with polynomial functions ensures that the saddle point system (12c) is invertible, or equivalently, the interpolation system is well-defined. The thin plate splines so represent a *conditionally* positive definite set of functions of order L, i.e., for any set of centers $\{x_i\}_{i=1}^{N}$ satisfying $\sum_{i=1}^{N} \alpha_i p(x_i) = 0$ for any polynomial p in the span of $\{p_l\}_{l=1}^{L}$, the quadratic form $\sum_{i=1}^{N} \sum_{j=1}^{N} \alpha_i \alpha_j \varphi(\|x_i - x_j\|)$ is positive.

The local Lagrange functions provide approximation rates analogous to well-known approximation rates for Lagrange functions, which are globally supported. We will exploit this result to establish an L^2 error estimate for the interpolant determined via a conforming basis of local Lagrange functions, see Proposition 1.

Lemma 1. *Let n and m denote the space dimension and thin plate spline parameter* (12b)*, respectively. Suppose that $n < 2k \leq 2m$ and $f \in W_2^k(\Omega \cup \Omega_I)$ satisfies $f|_{\Omega_I} = 0$. Then, for sufficiently large M associated with Υ_i given by* (11b)*, the quasi-interpolant*

$$\tilde{I}_X(f) = \sum_{i=1}^{N} f(x_i) b_i\,,$$

satisfies

$$\|f - \tilde{I}_X f\|_{L^2(\Omega)} \leq C h^k \|f\|_{W_2^k(\Omega)}.$$

Proof. We assume the set of centers $\Xi \subset \Omega \cup \Omega_I$ with $X := \Xi \cap \Omega$. Let χ_i be the Lagrange functions centered at x_i and b_i denote the local Lagrange function

centered at x_i. Then,

$$\|u - \sum_{i=1}^{N} u(x_i) b_i\|_{L^2(\Omega\cup\Omega_I)} \leq \|u - \sum_{i=1}^{N} u(x_i)\chi_i\|_{L^2(\Omega\cup\Omega_{\mathcal{I}})} + \|\sum_{i=1}^{N} u(x_i)(\chi_i - b_i)\|_{L^2(\Omega\cup\Omega_I)}.$$

Since $\sum_{i=1}^{N} u(x_i)\chi_i$ is the Lagrange function interpolant to u using the set of centers in $xi \subset \Omega\cup\Omega_I$, we apply [10, Thm 4.2] to $\Omega\cup\Omega_I$ to obtain the estimate

$$\|u - \sum_{i=1}^{N} u(x_i)\chi_i\|_{L^2(\Omega\cup\Omega_I)} \leq Ch^k \|u\|_{W_2^k(\Omega\cup\Omega_I)}\,.$$

Next, we apply [9, Theorem 4.10] to bound $\|b_x i - \chi_x i\|_{L^2(\Omega\cup\Omega_I)}$. Because $N \leq Cq^{-d}$ holds for quasi-uniformly distributed sets and applying the Sobolev embedding theorem to bound $\|u\|_{L^\infty(\Omega\cup\Omega_I)} \leq C\|u\|_{W_2^k(\Omega\cup\Omega_I)}$, grants the estimate

$$\begin{aligned}\|\sum_{i=1}^{N} u(x_i)(b_i - \chi_i)\|_{L^2(\Omega\cup\Omega_I)} &\leq Cq^{-n}\|u_i\|_{\ell^2(N)} \sup_i \|b_i - \chi_i\|_{L^2(\Omega\cup\Omega_I)} \\ &\leq q^{-2n}\|u\|_{L^\infty(\Omega\cup\Omega_I)} h^{M\nu\backslash 2-4m+2n-2\tau-1} \\ &\leq Ch^{M\nu\backslash 2-4m-2\tau-1}\|u\|_{W_2^k(\Omega\cup\Omega_I)}.\end{aligned}$$

Therefore, for sufficiently large M, the exponent on h is at least as large as k. Combining the two inequalities yields the desired result.

3.2. Local Lagrange Quadrature

We introduce a quadrature method that is essential for the implementation of the Galerkin method we introduce in Section 4. Let $f \in W_2^\beta(\Omega)$ satisfy $f|_{\Omega_{\mathcal{I}}} = 0$ and let $X \subset \Omega$ be a collection of N centers. Let χ_i be a globally supported Lagrange function centered at $x_i \in X$ and let b_i be a local Lagrange function centered at x_i. We define the quadrature weight at x_i to be $w_i = \int_\Omega \chi_i(x)\,dx$ and the *Lagrange function quadrature rule* to be $Q_X(f) = \sum_{i=1}^{N} f(x_i)w_i$. Similarly, we define the *local* quadrature weight at x_i and *local* quadrature method to be

$$\hat{w}_i = \int_\Omega b_i(x)\,dx \;\text{ and }\; \hat{Q}_X(f) = \sum_{i=1}^{N} f(x_i)\hat{w}_i\,, \tag{13}$$

respectively. We demonstrate that the quadrature error decreases as the mesh norm decreases.

Lemma 2. *Let n and m denote the space dimension and thin plate spline parameter* (12b)*, respectively. Suppose that $f \in W_2^k(\Omega)$ for $n < 2k \leq 2m$ satisfy $f|_{\Omega_{\mathcal{I}}} = 0$. Then, for sufficiently large M associated with Υ_i given by* (11b)*,*

$$\left|\int_\Omega f(x) - \hat{Q}_X(f)\right| \leq Ch^k \|f\|_{W_2^k(\Omega)}\,.$$

PROOF. The result follows by the Cauchy-Schwarz inequality and Lemma 1.

The Lagrange function quadrature rule was first proposed in [11] for boundaryless manifolds, e.g., a sphere. The quadrature method proposed enabled the use of arbitrarily scattered data samples for quadrature on spheres. Although the quadrature weights proposed required solving a dense linear system, the authors provided a preconditioner for the quadrature weight linear algebraic system that resulted in a practical quadrature routine [8, Section 7]. The Lagrange function quadrature routine has also been used for Galerkin methods for partial differential equations on spheres in [12]. In the paper [1], a quadrature rule for compact domains was introduced by modifying the construction on manifolds.

The local quadrature weights are constructed by computing the integrals of the translates $\varphi(\|x - x_i\|)$, a modification of the method of [1]. Substituting (12a) into (13) grants

$$\hat{w}_i = \sum_{j=1}^{|\Upsilon_i|} \alpha_j \int_\Omega \varphi(\|x - x_j\|)\, dx + \sum_{l=1}^{L} \beta_l \int_\Omega p_l(x)\, dx\,.$$

The construction of the local quadrature weights does not require the solution of a large linear system. However, the weights do require that the local Lagrange function coefficients are first computed.

4. Galerkin Radial Basis Function Method

4.1. Local Lagrange Discretization

Let $X \subset \Omega \cup \Omega_{\mathcal{I}}$ be a set of quasi-uniformly scattered centers with mesh norm h. For each center $x_i \in X$, we construct b_i (12a), the local Lagrange function centered at x_i. Unfortunately, the $\operatorname{span}\{b_i : x_i \in \Omega\} \not\subset L^2_c(\Omega \cup \Omega_{\mathcal{I}})$ because the local Lagrange functions b_i are necessarily nonzero over $\Omega_{\mathcal{I}}$. Hence we replace b_i with $\tilde{b}_i = b_i \mathbb{1}_\Omega$, where $\mathbb{1}_\Omega$ is an indicator function for Ω and set

$$V_h = \operatorname{span}\{\tilde{b}_i\}_{i=1}^N \subset L^2_c(\Omega \cup \Omega_{\mathcal{I}})\,, \tag{14}$$

the space of shape functions (9). By construction, a function $f^h \in V_h$ satisfies the constraint $f^h|_{\Omega_{\mathcal{I}}} = 0$. The following result explains that this constraint does not increase the approximation error when the constrained local Lagrange function $\tilde{b}_i$ replaces b_i. We remark that we can replace the constraint on $f^h \in V_h$ so that $f^h|_{\Omega_{\mathcal{I}}} = g$ for some function $g \in L^2(\Omega_{\mathcal{I}})$ by instead considering $b_i \mathbb{1}_\Omega + g \mathbb{1}_{\Omega_{\mathcal{I}}}$. This clever choice enables us to consider nonhomogenous volume-constrained nonlocal diffusion problems (3), i.e., the volume constraint $u = g$.

Proposition 1. *Let $u \in W_2^k(\Omega)$ for $n < 2k \leq 2m$ be the solution to the nonlocal problem* (6) *where m denotes the thin plate spline parameter* (12b)*, and let $u_h \in V_h$ be the solution to the discrete variational problem* (9) *where V_h is given by* (14)*. Then the estimate*

$$\|u - u_h\|_{L^2(\Omega \cup \Omega_{\mathcal{I}})} \leq C h^k \|u\|_{W_2^k(\Omega \cup \Omega_{\mathcal{I}})}.$$

holds for sufficiently small h and for sufficiently large M associated with Υ_i given by (11b)

PROOF. By setting $u_h = \sum_{i=1}^{N} u(x_i)\tilde{b}_i$, we have

$$\|u - u_h\|_{L^2(\Omega\cup\Omega_{\mathcal{I}})} \leq C\|u - \sum_{i=1}^{N} u(x_i)\tilde{b}_i\|_{L^2(\Omega\cup\Omega_{\mathcal{I}})} = C\|u - \sum_{i=1}^{N} u(x_i)b_i\|_{L^2(\Omega)}$$
$$\leq C\|u - \sum_{i=1}^{N} u(x_i)b_i\|_{L^2(\Omega\cup\Omega_{\mathcal{I}})}.$$

We now apply Lemma 1 to establish the estimate.

Section 2.1 demonstrated that the infinite dimensional nonlocal diffusion problem is well-posed subject to the conditions on the kernel. In particular, the nonlocal operator $\mathcal{L}$ (3) is a mapping from $L^2(\Omega \cup \Omega_{\mathcal{I}})$ to $L^2(\Omega)$. The error estimate then implies that the source term $f \in W_2^k(\Omega)$ in order to satisfy the hypotheses of the estimate. If $m = n = 2$, then k has an upper bound of 2; in other words, a quadratic convergence rate is possible when $\Omega \subset \mathbb{R}^2$ and $f \in W_2^2(\Omega)$. Our numerical experiments demonstrate second order convergence.

We now demonstrate that the condition number of the stiffness matrix $\mathbf{A}$ is bounded independent of the mesh norm h or the separation radius q. The Lemma that follows extends results available for finite element methods, e.g., [13], to RBF. The result relies on recent advances, see, e.g., [9], in the theory of radial basis functions.

Lemma 3. *The condition number of the discrete stiffness matrix $\boldsymbol{A}$ is bounded above by a constant independent of h and q.*

PROOF. Let $\mathbf{A}$ denote the $N \times N$ symmetric stiffness matrix and let $\mathbf{c} \in \mathbb{R}^n$. Then,

$$\langle \mathbf{Ac}, \mathbf{c} \rangle = \sum_{i=1}^{N} \left(\sum_{j=1}^{N} (\mathbf{A}_{i,j} c_i) c_j \right) = a\left(\sum_{i=1}^{N} c_i \tilde{b}_i, \sum_{j=1}^{N} c_j \tilde{b}_j \right).$$

By the coercivity and continuity of the bilinear form and since $\sum_{i=1}^{N} c_i \tilde{b}_i \in L_c^2(\Omega \cup \Omega_{\mathcal{I}})$, there exists λ_1, λ_2 such that

$$\lambda_1 \| \sum_{i=1}^{N} c_i \tilde{b}_i \|_{L^2(\Omega\cup\Omega_{\mathcal{I}})} \leq a\left(\sum_{i=1}^{N} c_i \tilde{b}_i, \sum_{j=1}^{N} c_j \tilde{b}_j \right) \leq \lambda_2 \| \sum_{i=1}^{N} c_j \tilde{b}_j \|_{L^2(\Omega\cup\Omega_{\mathcal{I}})}.$$

It follows that since $\tilde{b}_i = 0$ on $\Omega_{\mathcal{I}}$ and $\tilde{b}_i|_{\Omega} = b_i$,

$$\lambda_1 \| \sum_{i=1}^{N} c_i \tilde{b}_i \|_{L^2(\Omega\cup\Omega_{\mathcal{I}})} = \lambda_1 \| \sum_{i=1}^{N} c_i b_i \|_{L^2(\Omega)}.$$

By [9, Proposition 5.3] and [9, Theorem 4.12], there exists C_Ω and $C_{\Omega\cup\Omega_\mathcal{I}}$ independent of h and q such that

$$C_\Omega q^N \|\mathbf{c}\|_{\ell^2(N)} \le \|\sum_{i=1}^N c_i b_i\|_{L^2(\Omega)} \qquad \|\sum_{i=1}^N c_i b_i\|_{L^2(\Omega\cup\Omega_\mathcal{I})} \le C_{\Omega\cup\Omega_\mathcal{I}} q^N \|\mathbf{c}\|_{\ell^2(N)}.$$

Then, we bound

$$\mathrm{cond}(\mathbf{A}) \le \frac{\lambda_{\max}(\boldsymbol{A})}{\lambda_{\min}(\boldsymbol{A})} \le \frac{C_{\Omega\cup\Omega_\mathcal{I}}\lambda_2}{C_\Omega \lambda_1}.$$

4.2. Approximating the stiffness matrix by quadrature

A direct evaluation of the integrals for the bilinear form a results in a dense stiffness matrix. However, the local Lagrange function $\tilde{b}_k$ decays rapidly away from the center x_k. We now introduce a practical method to approximate the elements of the $\mathbf{A}$ that generates a sparse matrix. The method applies the quadrature rule (13) twice because of the double integration:

$$\begin{aligned}
\mathbf{A}_{i,j} &= a(\tilde{b}_i, \tilde{b}_j) \\
&= 2\int_{\Omega\cup\Omega_\mathcal{I}}\int_{\Omega\cup\Omega_\mathcal{I}} \tilde{b}_i(x)\tilde{b}_j(x)\gamma(x,y)\,dx\,dy \\
&\quad - 2\int_{\Omega\cup\Omega_\mathcal{I}}\int_{\Omega\cup\Omega_\mathcal{I}} \tilde{b}_i(x)\tilde{b}_j(y)\gamma(x,y)\,dx\,dy \\
&\approx 2\,\delta_{i,j}\,\hat{w}_i \int_{\Omega\cup\Omega_\mathcal{I}} \gamma(x_i,y)\,dy - 2\,\hat{w}_i\hat{w}_j\,\gamma(x_i,x_j)\,, \qquad (15)
\end{aligned}$$

where we invoked the symmetry of the kernel for the second equality and then repeatedly exploited the identity $\tilde{b}_j(x_k) = \delta_{j,k}$ from the discussion following (12c). The assumption (4) on the kernel that $\gamma(x,y) = 0$ for $\|x-y\| \ge \varepsilon$ then results in a stiffness matrix that is nonzero only within the region of nonlocality. The integral involving $\gamma(x_i,y)$ may be computed analytically for some kernels or by quadrature. The resulting stiffness matrix is symmetric, and also positive definite when the weights $\hat{w}_i$ are positive and

$$\int_{\Omega\cup\Omega_\mathcal{I}} \gamma(x_i,y)\,dy > \sum_{j\ne i} \hat{w}_j\,\gamma(x_i,x_j)\,.$$

The latter inequality implies that the approximate stiffness matrix is strictly diagonally dominant and so positive definite since it is also symmetric. The necessity of a positive $\hat{w}_i$ is apparent otherwise the associated diagonal element is negative and hence $\mathbf{A}$ cannot then be positive definite.

We now demonstrate that the density of nonzero elements in the stiffness matrix is bounded independent of the mesh norm h and separation radius q.

Lemma 4. *Let $\{X\}_{h,q}$ be a collection of quasi-uniformly distributed centers in $\mathbb{R}^n$. Then, the ratio of the number of nonzero entries per row to the total number of columns is bounded independent of h, q.*

PROOF. Fix $X := X_{h,q}$ and fix $x_i \in X$. Recall that $\|x_i - x_j\| \geq \varepsilon$, $\mathbf{A}_{i,j} = 0$ by (15). Let $N_i = \{x_j : \|x_j - x_i\| \leq \varepsilon\}$. Let C_n denote the constant so that a ball of radius r has volume $C_n r^N$. The number of nonzero entries on row i is the same as the cardinality of N_i, which we compute by estimating the number of centers in N_i. We bound the cardinality $|N_i|$ of N_i by noting that every center is separated by at least q, so

$$C_n\big(|N_i|\big)q^N = \cup_{x_j \in N_i}\mu\big(B_q(x_i)\big) \geq \mu\big(B_\varepsilon(x_i)\big) = C_n\varepsilon^N\,,$$

which implies $|N_i| \leq \varepsilon^N q^{-n}$. The density per row is computed by $\frac{|N_i|}{N} \leq \frac{\varepsilon^N q^{-n}}{N}$. We bound N since we may cover Ω with balls of radius h by $\Omega \subset \cup_{x_j \in X} B_h(x_j)$. Consequently, $\mu(\Omega) \leq N C_n h^N$, which implies

$$\frac{N_i}{N} \leq \frac{\varepsilon^N q^{-n}}{\mu(\Omega) C_n^{-n} h^{-n}} = \frac{C_n \varepsilon^N}{\mu(\Omega)} \frac{h^N}{q^N}\,.$$

The result follows by recalling that (10b) bounds the mesh ratio h/q.

We compute the values $\boldsymbol{b}_i$ from (9) by applying the local Lagrange function quadrature rule

$$\boldsymbol{b}_i \approx f(x_i)\hat{w}_i \mathbb{1}_\Omega(x_i)\,, \tag{16}$$

introduced in Section 4.1.

Let $\tilde{u}_h$ denote the solution to the discretized linear system assembled by quadrature from (15) and (16). We desire an estimate that predicts the convergence rate of $\tilde{u}_h$ to u in terms of h, as in Proposition 1. However, this requires a thorough analysis of the affect of quadrature on the solution to the resulting linear system of equations. By applying the triangle inequality and Proposition 1, we may estimate

$$\|u - \tilde{u}_h\|_{L^2} \leq \|u - u_h\| + \|u_h - \tilde{u}_h\|_{L^2} \leq Ch^k \|u\|_{W_2^k} + \|u_h - \tilde{u}_h\|_{L^2}.$$

Both u_h and $\tilde{u}_h$ are linear combinations of local Lagrange functions with coefficients $\{\alpha_i\}_{i=1}^N$ and $\{\tilde{\alpha}_i\}_{i=1}^N$ respectively. In the numerical experiments we present in Section 5, we only produce the coefficients $\{\tilde{\alpha}_i\}_{i=1}^N$ since we apply quadrature to assemble the linear system of equations. The error between u_h and $\tilde{u}_h$ may be quantified by

$$\|u_h - \tilde{u}_h\|_{L^2} = \|\sum_{i=1}^N (\alpha_i - \tilde{\alpha}_i) b_i\|_{L^2} \leq Cq^N \|\alpha_i - \tilde{\alpha}_i\|_{\ell^2(N)}.$$

We do not currently have an estimate to bound $\|\alpha_i - \tilde{\alpha}_i\|_{\ell^2(N)}$. Despite the lack of theoretical justification, we demonstrate in Section 5 that the discrete solution produced by solving the linear system assembled by using quadrature follows an estimate of the form in Proposition 1. These results suggest $\|u - \tilde{u}_h\|_{L^2} \approx \|u - u_h\|_{L^2} \leq Ch^k \|u\|_{W_2^k}$. Further theoretical work on RBF quadrature methods is required to resolve this estimate.

5. Numerical Results

We present numerical results for experiments using the discretization described in Section 4. We discuss local Lagrange function construction, L^2 error and condition number computations. We compare the theoretical prediction for L^2 convergence and condition numbers with observed results from numerical experiments. We consider solving two dimensional problems of the form (9) with a radial kernel Φ and two different diffusion coefficients κ; see Section 5.1 and Section 5.2. For all tests we consider zero Dirichlet volume constraints. The tests are computed on the set $\Omega \cup \Omega_{\mathcal{I}}$ where $\Omega = (0,1) \times (0,1)$ and $\Omega_{\mathcal{I}} = [-\frac{1}{4}, \frac{5}{4}] \times [-\frac{1}{4}, \frac{5}{4}] \backslash \Omega$. All computations are done in MATLAB and the condition numbers of the sparse stiffness matrices are approximated by the condest function. The sparse linear system is solved with either MATLAB's backslash operator or by conjugate gradient with a specified tolerance of 10^{-9}. The number of iterations required for the convergence of the conjugate gradient algorithm did not vary as the mesh norm decreased. This is as expected since the condition number does not change with the mesh norm.

The local Lagrange functions are constructed with linear combinations of the surface spline (12b) where $n = 2, L = 3$ and $m = 2$. Each local Lagrange function is constructed using approximately $11 \log N^2$ nearest neighbor centers, where N is the total number of centers in $\Omega \cup \Omega_{\mathcal{I}}$. The stiffness matrix for the nonlocal problem only requires Lagrange functions centered in Ω, although thin plate splines centered in $\Omega_{\mathcal{I}}$ are required for the construction of the local Lagrange functions as described in Section 3.1.

The kernel (7) is used and a solution $u \in L^2_c(\Omega \cup \Omega_{\mathcal{I}})$ is chosen for each numerical experiment. The source function f is manufactured by computing $\mathcal{L}u(x_i) = f(x_i)$ for each center x_i, the values of $f(x_i)$ are computed by using tensor products of Gauss-Legendre nodes to approximate the integral in (3).

We study L^2 convergence of the discrete solution by constructing sets of uniformly spaced centers and sets of scattered centers with various mesh norms. Uniformly spaced collections of centers X_h are constructed using grid spacing $h = .04, .02, .014, .008$, and $.006$. Collections of scattered centers $\tilde{X}_h$ are constructed by modifying centers in X_h by a random perturbation of magnitude at most $4h/15$. The convergence of the discrete solution u_h to the solution u is measured by plotting the L^2 norm of the error $\|u_h - u\|_{L^2(\Omega \cup \Omega_{\mathcal{I}})}$ against the mesh norm h. We expect for $u \in W_2^k(\Omega \cup \Omega_{\mathcal{I}})$ that $\|u - u_h\|_{L^2(\Omega)} \leq Ch^k \|u\|_{W_2^k(\Omega)}$ by Proposition 1.

5.1. Linear diffusion coefficient

We choose solution a u and a kernel γ with diffusion coefficient κ and radial function Φ given by

$$\begin{cases} u(x_1, x_2) = \sin(2\pi x_1) \sin(2\pi x_2) \mathbb{1}_{\Omega}(x_1, x_2) \\ \kappa(x_1, x_2) = 1 + x_1 + x_2 \\ \Phi_\varepsilon(\|x - y\|) = \exp\left(-(1 - \varepsilon^{-2} \|x - y\|^2)^{-1} \right). \end{cases} \tag{17}$$

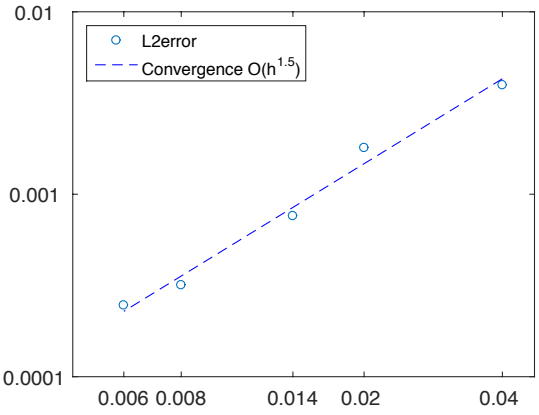

Figure 2: The log of h versus the log of the L^2 error for the linear diffusion coefficient experiment with functions given by (17) is displayed.

Figure 2 displays the observed L^2 convergence rates with respect to the mesh norm h for the uniformly spaced and scattered centers experiments. The log of the computed L^2 error versus the log of the mesh norm is presented along with a best fit line to estimate the convergence order of the observed data. Table 1 displays the condition numbers of the discrete stiffness matrices. The observed condition numbers of the stiffness matrices do not increase as the mesh norm decreases, which matches the result of Lemma 3.

5.2. Exponential diffusion coefficient

We choose solution a u and a kernel γ with diffusion coefficient κ and radial function Φ given by

$$\begin{cases} u(x_1,x_2) = \big(x_1(x_1-1)\big)^{\frac{3}{2}}\big(x_2(x_2-1)\big)^{\frac{3}{2}}\mathbb{1}_\Omega(x_1,x_2) \\ \kappa(x_1,x_2) = \exp(x_1+x_2) \\ \Phi_\varepsilon(\|x-y\|) = \exp\big(-(1-\varepsilon^{-2}\|x-y\|^2)^{-1}\big)\,. \end{cases} \tag{18}$$

Figure 3 displays the L^2 convergence plots for the experiments involving u_2 and κ_2. The L^2 error rate matches the expected convergence rate predicted by Proposition 1. The expected h^2 order convergence is observed in both the uniformly spaced centers and the scattered centers experiments. Table 1 displays the condition numbers for the discrete stiffness matrices of various values for h. The condition numbers of the discrete stiffness matrices do not increase as the mesh norm decreases, which matches the prediction in Lemma 3.

5.3. Vanishing Nonlocality

We present numerical results investigating the effects of decreasing the nonlocality ε. As discussed following (8), the solution of the nonlocal problem

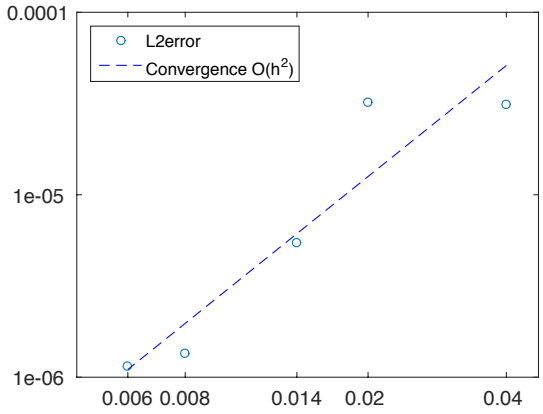

Figure 3: The log of h versus the log of the L^2 error for the exponential diffusion coefficient experiment with functions given by (18) is displayed.

Table 1: The mesh norm h, number of rows n of the stiffness matrix, and the estimated condition number for the stiffness matrix with the linear diffusion coefficient (17) and the exponential diffusion coefficient (18). The condition numbers of the stiffness matrices does not increase as h decreases.

		Approximate Condition Number	
h	n	Linear	Exponential
2.83e-2	625	58	89
1.41e-2	2500	59	90
9.9e-3	5041	59	90
5.7e-3	15625	60	92
4.2e-3	27889	60	92

converges to the solution of the classical diffusion equation with coefficient κ as ε decreases. Recent work has investigated the effects of balancing the mesh ratio h for a finite element discretization with decreasing ε to some limit, e.g., 0. The authors of [14, Section 4.3] demonstrated that as the nonlocality decreases to zero while hold the mesh size fixed, the finite element stiffness matrices for the nonlocal problems converged to discretizations of the local problem. More abstractly, a thorough study on asymptotically compatible schemes extended the previous work to general discretizations such as collocation, finite difference, and Galerkin methods [15]. Our objective here is to investigate, for fixed mesh norm h, how the solution to a nonlocal problem with decreasing nonlocality ε compares to the solution to the corresponding local problem, similar to [14, Section 4.3]. As the RBF method we present is a new method not previously considered, we perform similar experiments to understand whether this method behaves analogously as the methods considered in [14] behave in the local limit.

We consider inhomogeneous kernels of the form

$$\gamma_\varepsilon(x,y) = \frac{1}{\varepsilon^3}\big(\kappa(x)+\kappa(y)\big)\Phi_\varepsilon(\frac{1}{\varepsilon}\|x-y\|)\,. \tag{19}$$

We investigate approximating the solution to an inhomogeneous differential equation by solving an inhomogeneous nonlocal problem with sufficiently small ε. Our numerical experiments demonstrate that the discrete solution to the inhomogeneous nonlocal problem converges to the solution of the inhomogeneous differential equation.

We assume that $\kappa, u : \mathbb{R} \to \mathbb{R}$ are smooth functions. Then, for fixed $x \in \Omega$, we apply a Taylor series expansion in a ball $B_\varepsilon(x)$ for $u(y)-u(x)$ and $\kappa(x)+\kappa(y)$ to $\mathcal{L}$ to obtain

$$\mathcal{L}_\varepsilon u(x) = 2\big(k(x)u'(x)\big)' \int_{-1}^{1} \tau^2 \Phi_\varepsilon(|\tau|)d\tau + O(\varepsilon^2)\,,$$

where we invoked the symmetry (in x and y) of the kernel (19). Therefore, as ε decreases to zero,

$$\mathcal{L}_\varepsilon u(x) \to \big(\rho k(x)u'(x)\big)' \text{ and } \rho := 2\int_{-1}^{1} \tau^2 \Phi(|\tau|)\,d\tau\,,$$

a formal derivation of (8).

We numerically experiment with a Lagrange function discretization to solve the problem $\mathcal{L}_\varepsilon u_\varepsilon = f$ for inhomogeneous nonlocal operators. Let u denote the solution to the classical problem (8) and let h be a given mesh norm. We solve $\mathcal{L}_\varepsilon u_\varepsilon = f$ by discretizing the problem with Lagrange functions to construct an approximate solution $u_{\varepsilon,h}$. We numerically demonstrate that as $\varepsilon \to 0$, $\|u - u_{\varepsilon,h}\|_{L^2(\Omega\cup\Omega_\mathcal{I})} \approx O(\varepsilon^2)$.

We let $\Phi(\varepsilon^{-1}\|x\|) = \big(1-\varepsilon^{-2}\|x\|^2\big)\mathbb{1}_{\|x\|<\varepsilon}(x)$ and we consider two diffusion coefficients $\kappa(x,y)$. We first consider a case of a linear inhomogeneous function of the form $\kappa_1(x,y) = 1+x+y$ and $\kappa_2(x,y) = \exp(x+y)$. We set γ_ε as

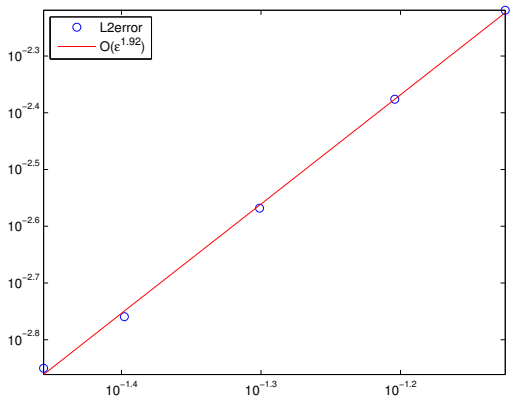

Figure 4: The log of ε vs. the log of the L^2 error of the discrete solution $u_{\varepsilon,h}$ is plotted for the experiment using κ_1. As ε goes to zero, we observe ε^2 convergence.

in (19) with the two choices for κ. The mesh norm $h = .000075$ is fixed for the experiments and we consider a range of ε values from $.075, .0625, .05, .04$, and $.035$. We discretize the problem $\mathcal{L}_\varepsilon u_\varepsilon = f$ with Lagrange functions and a discrete solution $u_{\varepsilon,h}$ is computed as described in Section 4.

We choose

$$u(x) = \big(1 - \cos(2\pi x)\big)\mathbb{1}_{[0,1]}(x) \tag{20}$$

and we analytically compute the source term f for the classical problem (8) to obtain

$$f(x) = \begin{cases} -2\pi\big(\sin(2\pi x) + 2\pi(1+x)\cos(2\pi x)\big) & \text{for } \kappa_1\,, \\ -\exp(x)\big(2\pi\sin(2\pi x) + 4\pi^2\cos(2\pi x)\big) & \text{for } \kappa_2\,. \end{cases}$$

In contrast to the experiments in Section 5.1 and Section 5.2, the source function f is fixed, h is fixed, and ε changes. For the fixed collection of centers with $h = 7.5 \times 10^{-5}$, for either κ_1 or κ_2, the L^2 error $\|u - u_{\varepsilon,h}\|_{L^2[0,1]}$ converges at approximately the expected rate of $O(\varepsilon^2)$. A convergence rate of 1.94 was observed for κ_1 and 1.92 for κ_2. The numerical results support the contention that the solution to the classical problem (8) is approximated by discretizing and solving an inhomogeneous nonlocal volume constrained equation.

5.4. Effects of Scattering Centers on the Solution

We investigate the effects of using increasingly scattered collections of centers on the Galerkin radial basis function method. Radial basis function methods, being inherently meshfree, offer the possibility of working with highly nonuniform collections of centers. However, the mesh ratio ρ (10a) may become large for highly scattered collections of centers. This may have deleterious effects on the quadrature weights, the condition number of the stiffness matrix,

Table 2: Results for the scattered centers experiment. Larger values of scattering produces large mesh ratios, which may produce negative quadrature weights.

α	Mesh Ratio ρ	Condition Number	$\min_i \hat{w}_i$
$\frac{1}{16}$	1.142	7.9×10^1	3.34×10^{-4}
$\frac{2}{16}$	1.3	8.8×10^1	2.9×10^{-4}
$\frac{3}{16}$	1.6	9.0×10^1	2.0×10^{-4}
$\frac{4}{16}$	2.0	1.1×10^2	1.4×10^{-4}
$\frac{5}{16}$	2.7	1.4×10^2	4.4×10^{-5}
$\frac{6}{16}$	3.9	6.5×10^2	-7.6×10^{-5}
$\frac{7}{16}$	7.4	7.3×10^2	-2.1×10^{-4}

or the solution to the nonlocal problem. For example, the constants C_Ω and $C_{\Omega\cup\Omega_\mathcal{I}}$ in Lemma 3 implicitly depend upon the mesh ratio being bounded. Consequently, if the mesh ratio increases, Lemma 3 may not hold. Informally, a large value of ρ is analogous to a finite element discretization where one triangle becomes disproportionately small relative to the rest of the mesh.

We place uniformly spaced centers, X, with grid spacing $h = .02$ along $[-.25, 1.25]^2$. For each center in $[0, 1]$, a local Lagrange function will be generated. The centers outside of $[0, 1]^2$ are used only to aid in the later construction of the local Lagrange functions after we scatter the centers. A scattering parameter α is introduced, which will vary for each run of the experiment. Each center $x_i \in [0, 1]^2 \cap X$ is perturbed in a random direction with magnitude $\alpha \cdot h$ to generate the collection of scattered centers, X_α. The local Lagrange functions are then constructed, and the nonlocal problem is solved using the resulting discretization and quadrature weights. Our objective is to study how the condition number of the matrix, the mesh ratio ρ, and the quadrature weights vary as the scattering parameter α increases.

We choose values $\alpha = [1/16, 2/16, 3/16, 4/16, 5/16, 7/16]$. To prevent possible overlap of two centers after perturbing, we exclude the case $\alpha = 1/2$. For each value of α, a collection of scattered centers is generated and corresponding local Lagrange functions and quadrature weights are produced. We then solve the nonlocal problem with the method of Section 4.

The results of the experiment are listed in Table 2. Larger mesh ratio values indicate that two centers may be disproportionately close relative to the positions of other centers. In this case, the integrals of the local Lagrange functions may be negative which results in negative quadrature weights. As explained following (15), the resulting stiffness matrix is then no longer positive definite. While the resulting linear system may have a numerical solution, the conjugate gradient iteration may fail. As can be seen in Table 2, the cases of $\alpha = 6/16, 7/16$ results in negative quadrature weights.

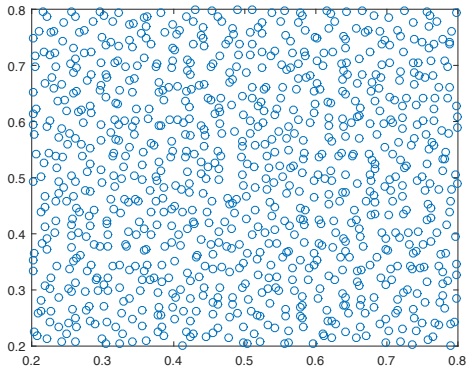

Figure 5: Example of randomly generated scattered centers perturbed with scatter parameter $\alpha = \frac{7}{16}$.

6. Conclusion

The primary contribution of our paper was the introduction of a meshfree discretization for a nonlocal diffusion problem using a localized basis of radial basis functions. Our method consisted of a conforming radial basis of local Lagrange functions for a variational formulation of a volume constrained nonlocal diffusion equation. We also established an L^2 error estimate on the local Lagrange interpolant. The stiffness matrix was assembled by a special quadrature routine unique to the localized basis. Combining the quadrature method with the localized basis produced a well-conditioned, sparse, symmetric positive definite stiffness matrix. We demonstrated that both the continuum and discrete problems are well-posed by appealing to recent work and presented numerical results for the convergence behavior of the radial basis function method. Finally, we explored approximating the solution to inhomogeneous classical diffusion equation by solving an inhomogeneous nonlocal integral equation using our proposed radial basis function method.

[1] S. D. Bond, R. B. Lehoucq, S. T. Rowe, A Galerkin radial basis function method for nonlocal diffusion, in: M. Griebel, M. A. Schweitzer (Eds.), Meshfree Methods for Partial Differential Equations VII, Vol. 100 of Lecture Notes in Computational Science and Engineering, Springer International Publishing, 2015, pp. 1–21.

[2] Q. Du, M. Gunzburger, R. B. Lehoucq, K. Zhou, Analysis and approximation of nonlocal diffusion problems with volume constraints, SIAM Review 54 (4) (2012) 667–696.

[3] N. Burch, M. DElia, R. Lehoucq, The exit-time problem for a Markov jump process, The European Physical Journal Special Topics 223 (14) (2014)

3257–3271.
URL http://dx.doi.org/10.1140/epjst/e2014-02331-7

[4] Q. Du, M. Gunzburger, R. B. Lehoucq, K. Zhou, A nonlocal vector calculus, nonlocal volume-constrained problems, and nonlocal balance laws, Math. Models Methods Appl. Sci 23 (2013) 493–540.

[5] Q. Du, R. Lehoucq, A. Tartakovsky, Integral approximations to classical diffusion and smoothed particle hydrodynamics, Computer Methods in Applied Mechanics and Engineering 286 (2015) 216–229.

[6] H. Wendland, Scattered Data Approximation, Cambridge University Press, 2005.

[7] G. E. Fasshauer, Meshfree Approximation Methods with MATLAB, World Scientific, 2007.

[8] E. J. Fuselier, T. Hangelbroek, F. J. Narcowich, J. D. Ward, G. B. Wright, Localized bases for kernel spaces on the unit sphere, SIAM J. Numer. Anal. 51 (5).

[9] T. Hangelbroek, F. J. Narcowich, C. Rieger, J. D. Ward, An inverse theorem for compact Lipschitz regions in $\mathbb{R}^d$ using localized kernel bases, ArXiv e-printsarXiv:1508.02952.

[10] F. J. Narcowich, J. D. Ward, H. Wendland, Sobolev error estimates and a Bernstein inequality for scattered data interpolation via radial basis functions, Constructive Approximation 24 (2) (2006) 175–186.

[11] E. J. Fuselier, T. Hangelbroek, F. J. Narcowich, J. D. Ward, G. B. Wright, Kernel based quadrature on spheres and other homogeneous spaces, Numerische Mathematik 127 (1) (2014) 57–92.

[12] F. J. Narcowich, S. T. Rowe, J. D. Ward, A Novel Galerkin Method for Solving PDEs on the Sphere Using Highly Localized Kernel Bases, ArXiv e-printsarXiv:1404.5263.

[13] K. Zhou, Q. Du, Mathematical and numerical analysis of linear peridynamic models with nonlocal boundary conditions, SIAM Journal of Numerical Analysis 48 (2010) 1759–1780.

[14] X. Tian, Q. Du, Analysis and comparison of different approximations to nonlocal diffusion and linear peridynamic equations, SIAM Journal of Numerical Analysis 51 (2013) 3458–3482.

[15] X. Tian, Q. Du, Nonconforming discontinuous galerkin methods for nonlocal variational problems, SIAM Journal of Numerical Analysis 53 (2014) 762–781.